第32卷第12期 焊 接 学 报 Vol. 32 No. 12
2011年12月 TRANSACTIONS OF THE CHINA WELDING INSTITUTION December 2011

稀土元素 Nd 对 Sn3.8Ag0.7Cu 焊点组织与抗剪强度的影响

皋利利， 薛松柏， 王 博
(南京航空航天大学 材料科学与技术学院，南京 210016)

皋利利

摘 要：研究了微量稀土元素 Nd(0，0.05，0.5 质量分数，%) 的添加对 Sn3.8Ag0.7Cu/Cu 焊点再流焊与 150 ℃时效条件下焊点组织与抗剪强度的影响. 结果表明，适量 Nd (0.05%) 的添加可以明显增强微焊点的抗剪强度，改善焊点组织；降低时效过程中 SnAgCu/Cu 焊点界面化合物生长速率以及焊点内部基体中 Cu_6Sn_5 化合物的颗粒粗化速率，从而有利于提高微焊点长期服役过程中的可靠性. 时效过程中，SAC-0.05Nd 焊点力学性能下降速率较 SAC 焊点有所降低，而 SAC-0.5Nd 焊点由于稀土化合物 $NdSn_3$ 相的粗化，与 SAC 微焊点力学性能下降速率无明显差异.

关键词：稀土 Nd；锡银铜钎料；组织；抗剪强度
中图分类号：TG454 **文献标识码**：A **文章编号**：0253－360X(2011)12－0073－04

0 序 言

SnAgCu 无铅钎料由于较优的综合性能，已被作为传统 SnPb 钎料的替代品，广泛应用于电子行业中. 但是 SnAgCu 钎料在电子行业的应用也带来了一些新的挑战，一方面其润湿性能相对传统的 SnPb 钎料仍需进一步改善；另一方面，其钎焊温度相对传统的 SnPb 钎料有很大的提高，同时由于锡的含量很高，会导致钎焊过程的界面反应剧烈而在焊点中生成大量的金属间化合物，大块金属间化合物的存在会成为服役过程中裂纹的萌生点，从而导致接头失效[1,2]. 因此控制再流焊及时效过程中焊点界面反应层的过度生长是提高 SnAgCu 焊点可靠性的有效途径之一.

已有的研究表明，SnAgCu 钎料中微量稀土元素的加入能够明显改善钎料及焊点的性能. 如改善钎料的润湿性能[3－5]、细化钎料组织[6－8]、降低内部 Cu_6Sn_5 以及 Ag_3Sn 金属间化合物的尺寸[9,10]、抑制 SnAgCu/Cu 界面化合物的生长速度[11－13]，从而获得综合性能优良的新型 SnAgCu 无铅钎料. 而前期的研究[14]表明，稀土元素 Nd 的添加，能够显著改善 Sn3.8Ag0.7Cu 钎料的润湿性能、微观组织以及焊点力学性能. 因此，在前面研究工作基础之上，进一步研究高温(150 ℃)存储过程中，SnAgCu-xNd(x = 0，0.05，0.5 质量分数，%) 焊点抗剪强度以及钎料/铜界面化合物的变化.

收稿日期：2010－08－29
基金项目：大学生创新训练计划资助项目

1 试验方法

1.1 合金成分设计及试样制备

试验的原材料采用 99.9%(质量分数) 的锡、银、铜及稀土钕. 首先按照所需成分比例制备 SnAgCu(SAC) 熔融钎料，加热至 900 ℃并通入氮气保护，然后将稀土钕压入到熔融钎料中保温 4 h 并每隔 1 h 搅拌一次以保证钎料成分的均匀性，得到试验所需的钎料合金，具体合金成分见表 1.

表 1 钎料合金及成分(质量分数，%)
Table 1 Solders alloys and compositions

钎料合金	Sn	Ag	Cu	Nd
SAC	95.50	3.8	0.7	0
SAC-0.05Nd	95.45	3.8	0.7	0.05
SAC-0.5Nd	95.00	3.8	0.7	0.50

1.2 焊点抗剪强度试验

试验材料主要包括：(1) 0805 型矩形片式电阻元件；(2) FR-4 基板，焊盘结构为 Au/Ni/Cu；(3) SAC-xNd 钎料丝，成分见表 1. 采用电烙铁进行片式电阻钎焊，烙铁温度控制为 370 ℃，钎焊时间为 3 ~

5 s. 钎焊后，将焊点置于电阻炉中进行不同时间的 150 ℃恒温时效. 使用日本 Rhesca 公司 STR-1000 型微焊点强度测试仪进行焊点的抗剪强度测试，剪切测试示意图如图 1 所示.

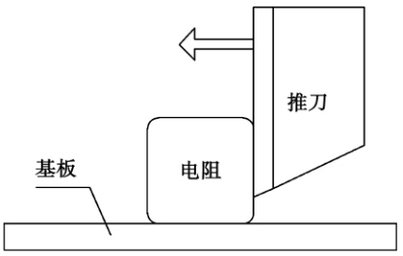

图 1 片式电阻剪切试验示意图

Fig. 1 Schematic diagram of shear force test

1.3 显微组织以及界面形貌观察

取表 1 中 SAC，SAC-0.05Nd 以及 SAC-0.5Nd 三种钎料合金在铜基板上进行铺展试验，钎焊温度为 250 ℃，保持时间为 60 s. 选取部分试样在电阻炉中进行不同时间的恒温时效，时效温度设置为 150 ℃. 将钎焊试样沿中心剖开，进行镶嵌、研磨并抛光，采用 4% HNO_3 + 酒精溶液对其进行腐蚀，观察焊点界面以及内部基体组织形貌.

2 试验结果及分析

2.1 稀土元素 Nd 对 SAC 无铅焊点力学性能影响

图 2 为表 1 中不同成分钎料再流焊及时效过程中片式电阻焊点剪切力的变化. 可以看出，无论再流焊或者时效过程中，SAC-0.05Nd 焊点均具有最优的力学性能，随着钕含量的增加，SAC-0.5Nd 焊点力学性能下降至低于 SAC 焊点. 并且，不同于 Li 等人[15]的研究结论，即稀土元素的加入能够显著降低时效过程中焊点力学性能的下降速率. 研究发现，

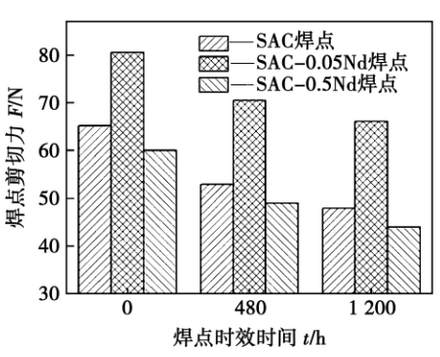

图 2 焊点抗剪切力

Fig. 2 Shear strength of solder joints

当稀土含量为 0.05% 时，相比 SAC 焊点，其力学性能的下降速率有所降低；但当稀土元素 Nd 为 0.5% 时，则对时效过程中 SAC 焊点力学性能下降速率影响甚微.

以上试验结果表明，适量稀土元素 Nd（0.05% 左右）的添加能够显著增强 SAC 焊点的力学性能，但过量稀土元素 Nd（0.5% 以上）的添加反而会恶化焊点的力学性能. 少量稀土元素 Nd 可以细化 SAC 无铅微焊点组织，添加过量则会形成粗大的 Sn-Nd 相. 细小均匀的组织有利于焊点力学性能的提高，粗大稀土相的存在则会恶化钎料的性能. 时效过程中，一方面，钕的加入显著抑制了钎料/铜界面化合物的生长，有助于焊点力学性能的保持；另一方面，时效过程中，稀土相 $NdSn_3$ 发生了不同程度的粗化，不利于焊点的力学性能的保持.

2.2 稀土元素 Nd 对 SAC 无铅焊点微观组织的影响

钎焊过程中，形成一定厚度的界面层是焊点具备良好冶金结合的重要标志，但过厚会严重恶化焊点的性能. 图 3 为三种焊点对应的界面组织形貌，图 3a 为 SAC/Cu 界面组织，依附界面化合物层以及焊点内部均有大块的金属间化合物产生，见 A 点. 能谱分析发现，大块的金属间化合物相为 Ag_3Sn 相. 这种大块的金属间化合物的存在，会对焊点的可靠性产生不利的影响. 图 3b 为 SAC-0.05Nd/Cu 界面组织，可以发现，其界面化合物层的厚度小于 SAC/Cu 焊点，焊点内部的金属间化合物也得到了一定程度的细化以及均匀化，细小、均匀分布的金属间化合物有利于焊点力学性能的提高. 随着元素 Nd 含量增加至 0.5%（图 3c），其界面层厚度接近 SAC-0.05Nd 焊点，但焊点内部出现了较大尺寸的 $NdSn_3$ 相，见 B 点，其 $NdSn_3$ 的存在将会对焊点的力学性能产生不利的影响. 稀土元素 Nd 具有一定的“亲锡效应”，加入后可以优先与锡结合，降低锡的活度，从而降低了界面化合物 Cu_6Sn_5 的生长驱动力.

图 4 为 SAC-xNd/Cu 焊点 150 ℃时效 720 h 的界面组织形貌. 由图 4 可以发现，时效 720 h 后，SAC-0.05Nd/Cu 以及 SAC-0.5Nd/Cu 界面层厚度明显小于 SAC/Cu 界面层厚度，时效后焊点的界面组织逐步变得平滑. 试验结果表明，适量元素 Nd（0.05%）的加入能够明显抑制 SAC/Cu 焊点界面化合物的生长速度，有利于焊点力学性能的保持；但由图 4c 可以发现当稀土元素 Nd 增至 0.5% 时，焊点中的稀土 $NdSn_3$ 相也发生了一定程度的聚集、粗化现象，不利于焊点力学性能的保持. 因此 SAC 钎料中钕的合适添加含量应控制在 0.05% 左右，钎料具有最佳的综合性能.

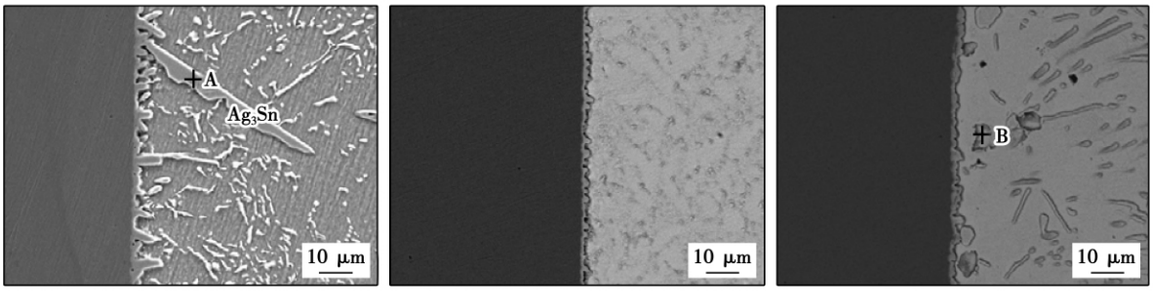

(a) SAC/Cu　　(b) SAC-0.05Nd/Cu　　(c) SAC-0.5Nd/Cu

图 3　SAC-*x*Nd/Cu 焊点再流焊界面组织

Fig. 3　As-reflowed interfacial microstructure of SAC-*x*Nd/Cu joints

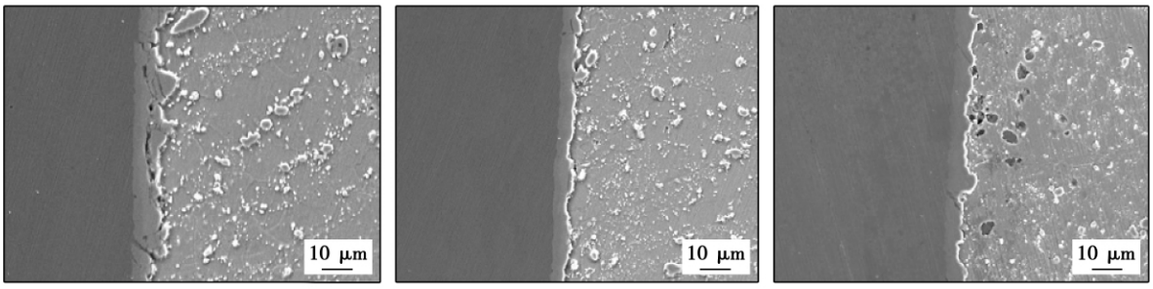

(a) SAC/Cu　　(b) SAC-0.05Nd/Cu　　(c) SAC-0.5Nd/Cu

图 4　SAC-*x*Nd/Cu 焊点时效 720 h 界面组织

Fig. 4　Interfacial microstructures of SAC-*x*Nd/Cu joints after 720 h aging

2.3　焊点内部化合物颗粒的粗化

图 5 为 SAC-*x*Nd/Cu 焊点时效 720 h 后的焊点内部钎料基体组织形貌，随着时效过程中焊点界面层厚度的增加，焊点的内部金属间化合物颗粒也发生了不同程度的粗化，颗粒粗化以 Cu_6Sn_5 化合物颗粒为主. 近似认为时效过程中，铜基板中铜的扩散主要贡献于界面化合物层的生长，而焊点内部基体中的 Cu_6Sn_5 化合物的新相体积不再增加，根据 Ostwald 熟化理论[16]，Cu_6Sn_5 化合物颗粒与锡基体之间界面能的降低为颗粒粗化的主要驱动力，而 Cu 原子在不同尺寸 Cu_6Sn_5 颗粒中具有不同的化学位，Cu_6Sn_5 颗粒尺寸越小，则其中铜的化学位越高. 时效过程中，由于小颗粒的不稳定性，造成小颗粒 Cu_6Sn_5 化合物中的 Cu 原子向尺寸较大的颗粒扩散，最终小颗粒消失，大颗粒长大.

由图 5 可见，SAC-0.05Nd 以及 SAC-0.5Nd 焊点内部 Cu_6Sn_5 金属间化合物颗粒的粗化程度明显低于 SAC 焊点，随着 Nd 元素的加入，焊点内部基体组织变得更为均匀，化合物颗粒尺寸降低，一定程度上可以降低由于化合物尺寸差异引起的元素化学位

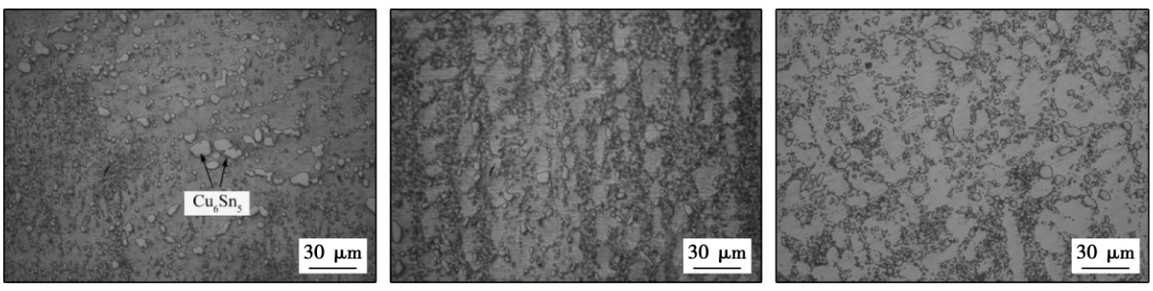

(a) SAC/Cu　　(b) SAC-0.05Nd/Cu　　(c) SAC-0.5Nd/Cu

图 5　SAC-*x*Nd/Cu 时效 720 h 焊点内部基体组织

Fig. 5　Matrix microstructures of SAC-*x*Nd/Cu joints after 720 h aging

梯度差，从而降低时效过程中金属间化合物颗粒粗化的驱动力，而钕的加入是否影响 SAC 焊点基体组织中 Cu 元素的扩散还需要进一步的研究.

3 结 论

(1) 微量稀土元素 Nd 的添加可以显著改善 SAC 钎料再流焊微焊点的力学性能. 时效过程中，SAC-0.05Nd 焊点力学性能下降速率相比 SAC 焊点有所降低，SAC-0.5Nd 焊点力学性能下降速率则与 SAC 相当.

(2) 钕的加入能够显著抑制再流焊及时效过程中 SAC/Cu 界面化合物的生长速度. 但时效过程中 SAC-0.5Nd/Cu 焊点中稀土 $NdSn_3$ 也发生了一定程度的粗化，对焊点力学性能产生不利的影响.

(3) 时效过程中，Nd 元素的加入，有效抑制了焊点内部基体中的金属间化合物颗粒(Cu_6Sn_5)的粗化.

参考文献:

[1] 张启运. 无铅钎料的困惑、前景与出路[J]. 焊接，2007(2)：6－10.
Zhang Qiyun. A puzzle in lead free soldering, its outlet and application prospect[J]. Welding & Joining, 2007(2): 6－10.

[2] Ho C E, Yang S C, Kao C R. Interfacial reaction issues for lead-free electronic solders[J]. Journal of Materials Science: Materials in Electronics, 2007, 18(1/3): 155－174.

[3] Yu D Q, Zhao J, Wang L. Improvement on the microstructure stability, mechanical and wetting properties of Sn-Ag-Cu lead-free solder with the addition of rare earth elements[J]. Journal of Alloys and Compounds, 2004, 376(1/2): 170－175.

[4] Hao H, Tian J, Shi Y W, *et al*. Properties of Sn3.8Ag0.7Cu solder alloy with trace rare earth element Y additions[J]. Journal of Electronic Materials, 2007, 36(7): 766－774.

[5] Shi Y, Tian J, Hao H, *et al*. Effects of small amount addition of rare earth Er on microstructure and property of SnAgCu solder[J]. Journal of Alloys and Compounds, 2008, 453(1/2): 180－184.

[6] Zhou Yinchun, Pan Qinglin, He Yunbin, *et al*. Microstructures and properties of Sn-Ag-Cu lead-free solder alloys containing La[J]. Transactions of Nonferrous Metals Society of China, 2007, 17: 1043s－1048s.

[7] Law C, Wu C, Yu D, *et al*. Microstructure, solderability, and growth of intermetallic compounds of Sn-Ag-Cu-RE lead-free solder alloys[J]. Journal of Electronic Materials, 2006, 35(1): 89－93.

[8] Dudek M, Sidhu R, Chawla N. Novel rare-earth-containing lead-free solders with enhanced ductility[J]. JOM Journal of the Minerals, Metals and Materials Society, 2006, 58(6): 57－62.

[9] 田 君，郝 虎，史耀武，*et al*. SnAgCuEr 系稀土无铅钎料的显微组织[J]. 焊接学报，2006，27(9)：31－34.
Tian Jun, Hao Hu, Shi Yaowu, *et al*. Microstructure of lead-free solder for a SnAgCuEr system[J]. Transactions of the China Welding Institution, 2006, 27(9): 31－34.

[10] Hao H, Shi Y, Xia Z, *et al*. Microstructure evolution of SnAgCu-Er lead-free solders under high temperature aging[J]. Journal of Electronic Materials, 2008, 37(1): 2－8.

[11] Dudek M A, Chawla N. Effect of rare-earth (La, Ce, and Y) additions on the microstructure and mechanical behavior of Sn-3.9Ag-0.7Cu solder alloy[J]. Metallurgical and Materials Transactions A, 2010, 41(3): 610－620.

[12] 周迎春，潘清林，李文斌，等. La 对 Sn-Ag-Cu 无铅钎料与铜钎焊接头金属间化合物的影响[J]. 中国有色金属学报，2008，18(9)：1651－1657.
Zhou Yingchun, Pan Qinglin, Li Wenbin, *et al*. Effect of La on intermetallic compounds of Sn-Ag-Cu lead-free alloy soldered with copper soldered with copper[J]. The Chinese Journal of Nonferrous Metals, 2008, 18(9): 1651－1657.

[13] Hao H, Tian J, Shi Y W, *et al*. Properties of Sn3.8Ag0.7Cu solder alloy with trace rare earth element Y additions[J]. Journal of Electronic Materials, 2007, 36(7): 766－774.

[14] Gao L L, Xue S B, Zhang L, *et al*. Effects of trace rare earth Nd addition on microstructure and properties of SnAgCu solder[J]. Journal of Materials Science-Materials in Electronics, 2010, 21(7): 643－648.

[15] Li G D, Shi Y W, Hao H, *et al*. Effect of rare earth addition on shear strength of SnAgCu lead-free solder joints[J]. Journal of Materials Science-Materials in Electronics, 2009, 20(2): 186－192.

[16] Snugovsky L, Perovic D D, Rutter J W. Experiments on the aging of Sn-Ag-Cu solder alloys[J]. Materials Science and Technology, 2004, 20(8): 1049－1054.

作者简介： 皋利利，女，1985 年出生，博士研究生. 主要从事微电子焊接及无铅钎料研究. 发表论文 6 篇. Email: gaolyly@126.com

通讯作者： 薛松柏，男，教授. Email: Xuesb@nuaa.edu.cn

Through comparing the simulation results and experimental measurements, the prediction accuracy of the developed thermo-elastic-plastic FEM based on Quick Welder was verified. Meanwhile, the influence of welding sequence on the residual stress distribution was clarified using numerical simulation method. The results show that both transverse residual stress and longitudinal residual stress were significantly affected by deposition sequence. The deposition sequence not only largely changes the peak values of residual stress, but also alters the shape of residual stress distribution.

Key words: numerical simulation; non-linear analysis; welding residual stress; welding sequence

Nanoindentation measurement of Sn-Cu-Ni joint WANG Jianxin, LAI Zhongmin, SUN Dandan (Province Key Lab of Advanced Welding Technology, Jiangsu University of Science and Technology, Zhenjiang 212003, China). p 59 - 62

Abstract: In order to study the effect of intermetallic compound on mechanical properties of joint, the elastic modulus and hardness of intermetallic compounds were analyzed by nanoindentation method, and the creep strain rate sensitivity of solder matrix was obtained by Mayo-Nix method. From the physical analysis of nanoindentation curves, the elastic modulu of $(Cu, Ni)_6Sn_5$ in Sn-Cu-Ni joints is 113.2 GPa ± 4.8 GPa, while the hardness is 5.59 GPa ± 0.32 GPa. It is found that intermetallic compounds are the key factors in the reliability of lead-free joints, due to the big contrasts between mechanical properties of intermetallic compounds and solder matrix. The creep strain rate sensitivities of Sn-Cu-Ni, Sn-Cu-Ni-0.05Ce and Sn-Pb solder matrix are 0.1286, 0.1248, and 0.1832, and the creep stress exponents are 7.7760, 8.0128, and 5.4585, respectively, which indicate the improvement in creep resistance of Sn-Cu-Ni joints due to Ce addition.

Key words: lead-free solder; nanoindentation; elastic modulu; creep strain rate sensitivity

Interfacial microstructure of sintering composites of PCBN grains-graphite particles-CuSnTi alloy ZHANG Bin, DING Wenfeng, XU Jiuhua, CHEN Zhenzhen, SU Honghua, FU Yucan (College of Mechanical and Electrical Engineering, Nanjing University of Aeronautics and Astronautics, Nanjing 210016, China). p 63 - 65, 69

Abstract: Sintering experiments of Cu-Sn-Ti alloy, polycrystalline cubic boron nitride (PCBN) abrasive grains and graphite particles were carried out at the heating temperature of 920 ℃ with the dwell time of 30 min. The strength of sintering bulks was measured by means of the three-point bending experiments. The interfacial microstructure and the phases of the sintering bulks were characterized using scanning electron microscope (SEM), energy dispersion spectrometer (EDS) and X-ray diffraction (XRD). The results reveal that in the case of the graphite content of 5 ~ 15 wt%, the bending strength of the composite bulks is above 91 MPa, which is much higher than that of the bulk strength of the vitrified grinding wheels. The elemental diffusion behavior has taken place across the joining interface between PCBN grains and Cu-Sn-Ti alloy in the sintering process. The compounds were formed, therefore, the PCBN grains were bonded firmly. Under such condition, the breakage of the PCBN grains has played the most important role in the fracture of the composite bulks. In particular, the breakage mode of the PCBN grains is the intergranular fracture.

Key words: PCBN abrasive grains; Cu-Sn-Ti alloy; bending strength; interfacial microstructure

Finite element analysis of temperature field during keyhole-plasma arc welding using SYSWELD software HU Qingxian[1], WANG Yanhui[1], YAO Qingjun[2], WANG Shunyao[1] (1. Provincial Key Lab of Advanced Welding Technology, Jiangsu University of Science and Technology, Zhenjiang 212003, China; 2. Jiangsu Province Special Equipment Safety Supervision Inspection Institute, Yangzhou Branch, Yangzhou 225003, China). p 66 - 69

Abstract: Considering the weld geometric characters of keyhole plasma arc welding (K-PAW), a suitable and adaptive combined heat source for numerical simulation is developed, i.e. at the transverse cross-section and along the workpiece thickness direction, the double-ellipsoidal volumetric heat source acts at upper part of the workpiece while a linearly-increased peak value of heat flux in gaussian cylinder mode exerts at lower part of the workpiece. Based on the developed adaptive combined heat source model, the welding temperature field of 6 mm thickness stainless steel is simulated by SYSWELD. The predicted weld geometry and fusion line locus at cross-section are in good agreement with the experimental measurement. This demonstrates the suitability of the combined volumetric heat source mode.

Key words: keyhole plasma arc welding; temperature field; combined volumetric heat source; finite element analysis

Study on ultrasonic stir hybrid welding of aluminum alloy HE Diqiu, LI Jian, LI Donghui, LIANG Jianzhang (State Key Laboratory of High-performance Complex Manufacturing, Central South University, Changsha 410083, China). p 70 - 72, 108

Abstract: Friction stir welding (FSW) of aluminum alloy usually results in a special "funnel shaped" temperature field, which makes obvious difference of microstructure properties in the direction of weld seams. In order to get better properties of welded joints, ultrasonic stir hybrid welding technology has been put forward in this paper, which concentrates the ultrasonic energy in deep weld seams through the stirring pin. Thickness of 2.5 mm 2219 aluminum alloy sheets has been adopted and welded by the two technologies mentioned above in this experiment, microstructure and mechanical properties of weld are analyzed and compared as well. Result shows that the weld joints of 2219 aluminum welded by the two technologies are both with good appearance and defect-free in the inner, and ultrasonic stir hybrid welding obviously has better mechanical properties.

Key words: ultrasonic stir hybrid welding; friction stir welding; 2219 aluminum alloy

Effect of Nd addition on microstructure and mechanical property of Sn3.8Ag0.7Cu solder joint GAO Lili, XUE Songbai, WANG Bo (College of Materials Science and Technology, Nanjing University of Aeronautics and Astronautics, Nanjing 210016, China). p 73 - 76

Abstract: The effects of Nd addition(0, 0.05, 0.5wt%) on the microstructure and shear strength of SAC solder joint under as-reflowed and 150 ℃ isothermal-aging process were investigated. Experimental results showed that Nd addition can obviously improve the shear strength and microstructure of the SAC solder joints. The growth rate of the SAC/Cu interfacial layer as

well as the coarsen rate of Cu_6Sn_5 particles in the Sn matrix during aging process was both restrained by Nd addition, which would enhance the reliability of the solder joint during service process. Moreover, during aging process, the shear strength reduction rate of SAC-0.05Nd solder joint was lower than that of SAC, but the shear strength reduction rate of SAC-0.5Nd solder joint showed no obvious difference compared with that of SAC because of the coarsen of $NdSn_3$ phase in aging process.

Key words: rare earth Nd; Sn3.8Ag0.7Cu solder; microstructure; shear strength

Microstructure of Mo-Cu alloy and 18-8 stainless steel joint by TIG with filler metal WANG Juan, LI Yajiang, ZHENG Deshuang, JIANG Qinglei (Key Laboratory for Liquid-Solid Structural Evolution & Processing of Materials, Ministry of Education, Shandong University, Jinan 250061, China). p 77 - 80

Abstract: The joining of Mo-Cu alloy with 18-8 stainless steel was carried out by tungsten inert-gas arc welding with filler wire. Microstructure, microhardness, element distribution and phase constituents near the fusion zone of Mo-Cu alloy/18-8 stainless steel joint were investigated by using optical microscopy, scanning electron microscop, microhardners and X-ray diffraction method. Results showed that there were mixed phases of martensite and austenite in the fusion zone at side of Mo-Cu alloy and austenite-ferrite dual phase in the weld metal and fusion zone near 18-8 stainless steel. The formation of carbonized layer in the fusion zone was promoted by the diffusion of Mo from Mo-Cu alloy to weld metal. The phase constituents near the fusion zone at side of Mo-Cu alloy were Mo, Cu, γ-Fe (Ni), $Fe_{0.54}Mo_{0.73}$ and $Cu_{3.8}Ni$. The existence of carbonized layer and $Fe_{0.54}Mo_{0.73}$ intermetallic compound resulted in a higher microhardness of 1 200 HV.

Key words: Mo-Cu alloy; 18-8 stainless steel; tungsten inert-gas arc welding with filler metal; microstructure

Laser lap welding of zinc-coated steel and 6016 aluminum alloy with Pb interlayer PENG Li, ZHOU Dianwu, WU Ping, ZHANG Yi, CHEN Genyu (State Key Laboratory of Advanced Design and Manufacturing for Vehicle Body, Hunan University, Changsha 410082, China). p 81 - 84

Abstract: The laser lap welding experiment with the Pb interlayer was carried out based on the DC56D + ZF galvanized steel of 1.2 mm and the 6016 aluminum alloy of 1.15 mm. The best appearance of welding were obtained by adjusting the welding parameters. By using optical microscopy, scanning electron microscopy, X-ray diffraction and the tensile test, mechanical properties of joints, fracture morphology and the main phase of the welded joint regional was studied. The results showed that when Pb interlayer was added in steel/aluminum, the average tensile strength and elongation of the steel/aluminum laser welding joints were 68.51 MPa and 2.37% respectively. Compared with that without Pb interlayer, the strength and alongation were improved significantly. The element distribution, phase composition and microstructure of the steel/aluminum interface were changed by the addtion of Pb interlayer. In the transition region of steel/aluminum joints, Fe, Al, Zn, Mg, Pb elements of the mixing zone width was larger, and a new ductile intermetallic compounds-Mg_2Pb was produced, which could improve the mechanical properties of weld metal.

Key words: laser welding; dissimilar metal; intermetallic compounds; microstructure

Effects of different solders on mechanical properties of micro-joints soldered with diode-laser soldering system LAI Zhongmin[1], ZHANG Liang[2], WANG Jianxin[1] (1. School of Materials Science & Engineering, Jiangsu University of Science and Technology, Zhenjiang 212003, China; 2. School of Mechanical & Electrical Engineering, Xuzhou Normal University, Xuzhou 221116, China). p 85 - 88

Abstract: Wettability of SnAgCu/SnAgCuCe solders on Cu substrate and properties of solder joints were tested by diode laser soldering system. The solder joints reliability during thermal cycling test was investigated by diode laser soldering system and IR reflow soldering method respectively. The results indicate that, as the laser output power increases, the spreading area of lead-free solder increases, the optimal wettability and spreadability are obtained while the laser output power increases to a certain range. Moreover, the results indicate that the wettability and spreadability of the two kinds of solders on Cu substrate are improved with the increase of heating time under the condition of selected laser output power. For QFP256 devices soldered with diode laser soldering system, optimum power can be found, the optimum power for SnAgCu solders is 16.7 W, for SnAgCuCe solders, it is 17 W. Moreover, during thermal cycling, the reliability of soldered joints obtained by diode laser soldering is higher than that by IR reflow soldering.

Key words: diode laser soldering system; wettability; laser output power; reliability

Fracture toughness of friction stir welded Invar 36 alloy at low temperature ZHAO Yue[1], WU Aiping[1], YUTAKA S. Sato[2], HIROYUKI Kokawa[2] (1. Key Laboratory for Advanced Materials Processing Technology, Ministry of Education, Department of Mechanical Engineering, Tsinghua University, Beijing 100084, China; 2. Department of Materials Processing, Graduate School of Engineering, Tohoku University, 6-6-02 Aramaki-aza-Aoba, Sendai 980-8579, Japan). p 89 - 92

Abstract: The fracture toughness of friction stir welded Invar36 alloy, obtained with travelling speed of 2 mm/s and rotational speed from 200 r/min to 1 000 r/min, were estimated at low temperature (77 K) by small punch test, and were compared with that at room temperature (298 K) as well. At 298 K, all welds have higher small punch energy than the base material. For the welds acquired with the same welding parameters, the small punch energy tested at 77 K is always higher than the ones at 298 K. The small punch energy of welds trends to increase with decreasing of the rotational speed at both 77 K and 298 K. With rotational speeds equal or less than 400 r/min, the small punch energy of welds is significantly higher than that of the base material at 77 K. The results indicate that the friction stir welds keep excellent ductility at low temperature. With the increase of travelling speed, higher heat input produces a coarser microstructure and leads to the reduction of fracture toughness in the weld.

Key words: Invar 36 alloy; friction stir welding; fracture toughness; small punch test

Optimization of parameters and joint microstructure of electrode beam welding of 2A14 Al alloy WANG Yarong,